BBA - Molecular Basis of Disease 1863 (2017) 2987–2998

Contents lists available at ScienceDirect

BBA - Molecular Basis of Disease

journal homepage: www.elsevier.com/locate/bbadis

Maternal insulin therapy does not restore foetoplacental endothelial dysfunction in gestational diabetes mellitus

Mario Subiabre[a], Luis Silva[a,b], Roberto Villalobos-Labra[a], Fernando Toledo[a,c], Mario Paublo[d], Marcia A. López[d], Rocío Salsoso[a,e], Fabián Pardo[a,f], Andrea Leiva[a], Luis Sobrevia[a,e,g,*]

[a] Cellular and Molecular Physiology Laboratory (CMPL), Division of Obstetrics and Gynaecology, School of Medicine, Faculty of Medicine, Pontificia Universidad Católica de Chile, Santiago 8330024, Chile
[b] Immunoendocrinology, Division of Medical Biology, Department of Pathology and Medical Biology, University of Groningen, University Medical Center Groningen (UMCG), Groningen, 9700 RB, The Netherlands
[c] Department of Basic Sciences, Faculty of Sciences, Universidad del Bío-Bío, Chillán 3780000, Chile
[d] Gynaecology and Obstetrics Service, Hospital San Juan de Dios, Santiago 8330024, Chile
[e] Department of Physiology, Faculty of Pharmacy, Universidad de Sevilla, Seville E-41012, Spain
[f] Metabolic Diseases Research Laboratory, Center of Research, Development and Innovation in Health - Aconcagua Valley, San Felipe Campus, School of Medicine, Faculty of Medicine, Universidad de Valparaíso, San Felipe 2172972, Chile
[g] University of Queensland, Centre for Clinical Research (UQCCR), Faculty of Medicine and Biomedical Sciences, University of Queensland, Herston, QLD 4029, Queensland, Australia

ARTICLE INFO

Keywords:
Diabetes
Insulin therapy
Endothelium
Arginine
Nitric oxide
Umbilical vein

ABSTRACT

Pregnant women diagnosed with gestational diabetes mellitus subjected to diet (GDM*d*) that do not reach normal glycaemia are passed to insulin therapy (GDM*i*). GDM*d* associates with increased human cationic amino acid transporter 1 (hCAT-1)-mediated transport of L-arginine and nitric oxide synthase (NOS) activity in foetoplacental vasculature, a phenomenon reversed by exogenous insulin. Whether insulin therapy results in reversal of the GDM*d* effect on the foetoplacental vasculature is unknown. We assayed whether insulin therapy normalizes GDM*d*-associated foetoplacental endothelial dysfunction. Primary cultures of human umbilical vein endothelial cells (HUVECs) from GDM*i* pregnancies were used to assay L-arginine transport kinetics, NOS activity, p44/42^{mapk} and protein kinase B/Akt activation, and umbilical vein rings reactivity. HUVECs from GDM*i* or GDM*d* show increased hCAT-1 expression and maximal transport capacity, NOS activity, and eNOS, and p44/42^{mapk}, but not Akt activator phosphorylation. Dilation in response to insulin or calcitonin-gene related peptide was impaired in umbilical vein rings from GDM*i* and GDM*d* pregnancies. Incubation of HUVECs *in vitro* with insulin (1 nmol/L) restored hCAT-1 and eNOS expression and activity, and eNOS and p44/42^{mapk} activator phosphorylation. Thus, maternal insulin therapy does not seem to reverse GDM*d*-associated alterations in human foetoplacental vasculature.

1. Introduction

Gestational diabetes mellitus (GDM) is a disease of pregnancy that characterizes by abnormal maternal D-glucose metabolism and altered insulin signalling in the foetoplacental circulation [1–5]. GDM-associated alterations lead to foetal hyperglycaemia and hyperinsulinemia resulting in endothelial dysfunction, and abnormal placental development and foetal growth [5,6]. Pregnant women that develop GDM are subjected to controlled diet (GDM*d* pregnancies) to reduce glycaemia to the recommended goals [1,4,7]. However, a fraction of these women does not reach normal glycaemia with diet and are passed to treatment with insulin (i.e., insulin therapy, GDM*i* pregnancies) until delivery [3,4,8–10]. Both the mother and newborns in GDM*d* and GDM*i* pregnancies show with normal glycaemia at term [11–13]. However, the foetoplacental endothelial cell function and vascular reactivity are altered in GDM*d* [3,5,13].

Increased expression and activity of the endothelial nitric oxide synthase (eNOS) and uptake of the amino acid L-arginine via the human

Abbreviations: GDM, Gestational diabetes mellitus; GDM*d*, Gestational diabetes mellitus treated with diet; GDM*i*, Gestational diabetes mellitus treated with diet and insulin; eNOS, Endothelial nitric oxide synthase; hCAT-1, Human cationic amino transporter 1; HUVECs, Human umbilical vein endothelial cells; NO, Nitric oxide; NOS, Nitric oxide synthase; eNOS, Endothelial nitric oxide synthase

* Corresponding author at: Cellular and Molecular Physiology Laboratory (CMPL), Division of Obstetrics and Gynaecology, School of Medicine, Faculty of Medicine, Pontificia Universidad Católica de Chile, P.O. Box 114-D, Santiago 8330024, Chile.
E-mail address: lsobrevia@uc.cl (L. Sobrevia).

http://dx.doi.org/10.1016/j.bbadis.2017.07.022
Received 21 April 2017; Received in revised form 29 June 2017; Accepted 24 July 2017
Available online 27 July 2017

cationic amino acid transporter 1 (hCAT-1), an isoform of human cationic amino acids transporters (hCATs) family [14,15], is reported in human umbilical vein endothelial cells (HUVECs) from GDM*d* pregnancies [13,16]. Exposure of HUVECs *in vitro* to physiological concentrations of insulin (up to 1 nmol/L) reverses the effects of GDM*d* on L-arginine transport [13] and NO synthesis [16]. Interestingly, high extracellular D-glucose (~25 mmol/L) also increases L-arginine transport via hCAT-1 and NO synthesis in HUVECs from normal pregnancies suggesting that hyperglycaemia could cause these changes in endothelial function [17]. Since insulin therapy results in normalization of the glycaemia in the mother and newborn at birth [4,9,18,19], a reversal of the effects of GDM*d* in the foetoplacental endothelial function is likely. In this study, we assayed whether maternal insulin therapy reverses the effects seen in GDM*d* on HUVECs function at birth. The results suggest that insulin therapy is not enough to reverse the foetoplacental endothelial dysfunction seen at birth in normoglycaemic, diet-controlled women with GDM.

2. Material and methods

2.1. Antibodies and materials

Primary monoclonal mouse *anti*-hCAT-1 and *anti*-ß-actin antibodies were from Sigma Aldrich (St Louis, MO, USA). Primary monoclonal mouse *anti*-eNOS phosphorylated at serine^{1177}, polyclonal rabbit *anti*-total p44/42^{mapk}, *anti*-phosphorylated p44/42^{mapk}, *anti*-total Akt and *anti*-phosphorylated Akt antibodies were from Cell Signaling Technology (Danvers, MA, USA). Primary monoclonal mouse *anti*-eNOS phosphorylated at threonine^{495} antibody was from BD Transduction Laboratories (San Jose, CA, USA). Primary monoclonal mouse *anti*-total eNOS antibody and secondary horseradish peroxidase-conjugated goat *anti*-rabbit or *anti*-mouse antibodies were from Santa Cruz Biotechnology (Santa Cruz, CA, USA). For isolation of HUVECs from umbilical cords Collagenase Type II from *Clostridium histolyticum* (Boehringer, Mannheim, FRG) was used. Medium M199, new born (NBCS) and fetal calf (FCS) sera, L-glutamine, and penicillin-streptomycin were from Gibco Life Technologies (Carlsbad, CA, USA). L-[^{3}H]Arginine and D-[^{3}H]mannitol were from NEN (Dreieich, FRG). N^G-Nitro-L-arginine methyl ester (L-NAME) and calcitonine gene related peptide (CGRP) were from Sigma Aldrich, and Akt Inhibitor IV (Inh-IV) and PD-98059 from Calbiochem (La Jolla, CA, USA). Immobilon-P polyvinylidene difluoride membranes was from BioRad Laboratories (Hertfordshire, UK). Qiagen RNAeasy kit was from Qiagen (Crawley, UK) and brilliant SYBR green qPCR Master Mix from Stratagene (La Jolla, CA, USA). The fluorescent dye 4-amino-5-methylamino-2′,7′-difluorofluorescein (DAF-FM) was from Molecular Probes (Leiden, The Netherlands).

2.2. Study groups

This study included samples collected from 13 full-term normal or 32 full-term GDM pregnancies from the Hospital Clínico UC-CHRISTUS (HCUC-C) and Hospital San Juan de Dios (HSJD) in Santiago de Chile. Pregnant women included in this study did not smoke or consume drugs or alcohol, and had no intrauterine infection or any other medical or obstetrical complications. Ethnicity of patients included in this study was Hispanic. The investigation conforms to the principles outlined in the Declaration of Helsinki. Ethics Committee approvals from the Faculty of Medicine of the Pontificia Universidad Católica de Chile and HSJD, and informed written consent of patients were obtained. All pregnant women with a normal glycaemia at the first trimester of pregnancy were evaluated by an oral glucose tolerance test (OGTT) with a unique glucose load (75 g fasting) at 24–28 weeks of gestation. Patients with basal glycaemia ≥ 5.56 (≥ 100 mg/dL, 8-9 h from last feeding in at least two different days) and with ≥ 7.9 mmol/L (≥ 140 mg/dL) at 2 h after glucose load at the second or third trimester of pregnancy were diagnosed with GDM (according to the Perinatal Guide 2015 report from the Health Ministry of Chile) [20]. Weight and body mass index (BMI) were recorded before pregnancy (i.e., pre-gestational) and for each trimester of pregnancy and at term.

Three groups of pregnant women were included in this study, i.e., normal pregnancies (n = 13), GDM*d* pregnancies (n = 14), or GDM*d* pregnancies where the mother was treated with insulin (GDM*i*, i.e., on insulin therapy) (n = 18). Qualified personnel of the HCUC-C and HSJD selected the groups of pregnant women according to their clinical characteristics following established protocols. Women coursing with normal pregnancies followed standard self-controlled diet and physical activity. Women with GDM*d* were subjected to dietary treatment with 1500 kcal/day and a maximum of 200 g per day carbohydrates. Plasma glucose was weekly measured at fasting and post-breakfast, before and 1 h after the midday and evening meals. Women with GDM*d* that did not reach normal glycaemia after two weeks of diet were passed into insulin therapy following protocols adopted at the Division of Obstetrics and Gynaecology at the HCUC-C and HSJD as recommended in the Perinatal Guide 2015 Chile [20]. In brief, women with GDM*d* not responsive to diet were treated for 8–10 weeks until delivery with two injections (one before breakfast and one at bedtime) of neutral protamine Hagerdon human insulin (Humulin-N or Insuman-N, 0.5–0.65 units/kg of pre-pregnancy body weight). Additional three injections of regular (rapid-acting) insulin (Humulin-R or Insuman-R) depending on pre-prandial self-controlled capillary glycaemia (0.1 to 6 units/kg per meal for 81–120 to > 250 mg/dL glucose, respectively) were administered to women with GDM*d* as described for insulin therapy in pregnant women with pre-gestational diabetes mellitus type 1 or 2 [11,21].

2.3. Human placenta and umbilical cords

Placentas were collected at delivery on ice and transferred to the laboratory until use 15–30 min later. Middle sections of umbilical cords (100–120 mm length) were dissected into 200 mL phosphate-buffered saline (PBS) solution (mmol/L: 130 NaCl, 2.7 KCl, 0.8 Na_2HPO_4, 1.4 KH_2PO_4, pH 7.4, 4 °C) until use 6–12 h later for isolation of endothelial cells.

2.4. Cell culture

HUVECs were isolated by collagenase digestion (0.25 mg/mL collagenase) from umbilical cords obtained at birth from normal, GDM*d*, or GDM*i* pregnancies and cultured (37 °C, 5% CO_2) in 1% gelatin-coated petri dishes (100 mm diameter) up to passage 3 in primary culture medium (PCM; M199 containing 5 mmol/L D-glucose, 10% NBCS, 10% FCS, 3.2 mmol/L L-glutamine and 100 U/mL penicillin-streptomycin). 16 h prior experiments the incubation medium was changed to M199 medium containing 0.25% NBCS and 0.25% FCS. Experiments were performed in the absence (hereafter referred as 'without insulin') or presence (8 h, hereafter referred as 'with insulin') of insulin (1 nmol/L), L-NAME (100 μmol/L, NOS inhibitor) [22], Inh-IV (1 μmol/L, protein kinase B/Akt inhibitor) [23], and/or PD-98059 (10 μmol/L, MAP kinase kinases 1/2 inhibitor) [24].

2.5. L-Arginine transport

Overall 0–1000 μmol/L L-arginine transport (3 μCi/mL L-[^{3}H]arginine, 1 min incubation, 37 °C) was measured in Krebs solution (mmol/L: 131 NaCl, 5.6 KCl, 25 $NaHCO_3$, 1 NaH_2PO_4, 20 Hepes, 2.5 $CaCl_2$, 1 $MgCl_2$, pH 7.4, 37 °C) as described [13]. Overall transport of L-arginine was defined as the result of the sum of a saturable component plus a nonsaturable, linear component of transport in the range of L-arginine concentrations used in this study (hereafter referred as a K_D value defined by $m \cdot [Arg]$, where m corresponds to slopes of lineal phases of transport at a given L-arginine concentration [*Arg*]) [13]. Cell

monolayers were rinsed with ice-cold Krebs to terminate tracer uptake.

Initial rate for transport (i.e., linear uptake up to 1 min) was derived from the slope of the linear phases of L-arginine transport. Values for transport were adjusted to the one phase exponential association equation considering the least squares fit:

$$v_i = V_m \bullet (1 - e^{-(k \bullet t)})$$

where v_i is initial velocity, V_m is mayor velocity at a given time (t) and L-arginine concentration, and e and k are constants. Overall L-arginine transport at initial rates was adjusted to the Michaelis-Menten hyperbola plus a nonsaturable, linear component (K_D) as described [13]. The saturable transport of L-arginine was derived by subtracting the $m \cdot [Arg]$ components from overall transport, and the transport kinetic parameters maximal velocity (V_{max}) and apparent Michaelis-Menten constant (K_m) of transport were calculated [13]. The relative contribution of GDM*d*, GDM*i*, insulin, PD-98059, or Inh-IV to the saturable L-arginine transport kinetic parameters was estimated from the maximal transport capacity (V_{max}/K_m) values for L-arginine transport by:

$$\frac{1}{{}^{C/X}F} = \frac{{}^{C}K \cdot {}^{X}V_{max}}{{}^{C}V_{max} \cdot {}^{X}K_m}$$

where ${}^{C}V_{max}$ and ${}^{C}K_m$ are the kinetics parameters for L-arginine transport in control conditions (i.e., in the absence of insulin, PD-98059, or Inh-IV) in cells from normal, GDM*d*, or GDM*i* pregnancies, and ${}^{X}V_{max}$ and ${}^{X}K_m$ are kinetics parameters of L-arginine transport in HUVECs from normal, GDM*d*, or GDM*i* pregnancies exposed to different experimental conditions [13,25]. Each transport assay was run in duplicate with transport activity expressed as pmol/μg protein/minute. Radioactivity in 0.5 N KCl cell digests was determined by liquid scintillation counting, and uptake was corrected for D-[^{3}H]mannitol disintegrations per minute (d.p.m.) in the extracellular space [13].

2.6. Western blotting

Total protein was obtained from confluent cells washed twice with ice-cold PBS and harvested in 100 μL of lysis buffer composed by 63.7 mmol/L Tris/HCl (pH 6.8), 10% glycerol, 2% sodium dodecylsulphate (SDS), 1 mmol/L sodium orthovanadate, 50 mg/mL leupeptin, and 5% 2-mercaptoethanol, as described [13]. Cells were sonicated (6 cycles, 5 s, 100 W, 4 °C), and total protein was separated by centrifugation (14,000*g*, 15 min, 4 °C). Proteins (70 μg) were separated by polyacrylamide gel (10%) electrophoresis and transferred onto Immobilon-P polyvinylidene difluoride membranes. The proteins were then probed against hCAT-1 (1:500 dilution, 12 h, 4 °C), total eNOS (1:500 dilution, 12 h, 4 °C), eNOS phosphorylated at serine^{1177} ($P\sim$Ser^{1177}-eNOS, 1:1000 dilution, 12 h, 4 °C), eNOS phosphorylated at threonine^{495} ($P\sim$Thr^{495}-eNOS, 1:1000 dilution, 12 h, 4 °C), total p44/42^{mapk} (1:1000 dilution, 3 h, room temperature), phosphorylated p44/42^{mapk} (1:1000 dilution, 3 h, room temperature), total Akt (1:1000 dilution, 3 h, room temperature), phosphorylated Akt (1:1000 dilution, 3 h, room temperature), and β-actin (1:3000, 1 h, room temperature). Membranes were rinsed in Tris buffer saline Tween and incubated (1 h) in TBS-T/0.2% BSA containing secondary horseradish peroxidase-conjugated antibodies. Proteins were detected by enhanced chemiluminescence (film exposure time was 1 min) in a ChemiDoc-It 510 Imagen System (UVP, LCC Upland, CA, USA) and quantified by densitometry [13].

2.7. Isolation of total RNA and reverse transcription

Total RNA was isolated using the Qiagen RNAeasy kit. RNA quality and integrity were insured by gel visualization and spectrophotometric analysis ($OD_{260}/_{280}$), quantified at 260 nm. Aliquots (2 μg) of total RNA were reversed transcribed into cDNA as described [13].

2.8. Quantitative RT-PCR

Experiments were performed using a StepOne Real-Time PCR system (Applied Biosystems, Foster City, CA, USA) in a reaction mix containing 0.5 μmol/L primers, and master mix provided in the brilliant SYBR green qPCR Master Mix as described [13]. SecureStartTaq DNA polymerase was activated (15 min, 95 °C), and the PCR cycling profile included a 95 °C denaturation (15 s), annealing (20 s) at 54 °C (hCAT-1 and 28S) or 60 °C (eNOS, insulin receptor A (IR-A), insulin receptor B (IR-B)), and extension at 72 °C for variable times (hCAT-1, 10 sec; eNOS, 17 sec; IR-A and IR-B, 20 sec; 28S, 10 s). Product melting temperature values were 79.1 °C (hCAT-1), 86.43 °C (eNOS), 87.2 °C (IR-A), 87.6 °C (IR-B), and 86.7 °C (28S). The oligonucleotide primers used in this study were: hCAT-1 sense: 5′-GAGTTAGATCCAGCAGACCA-3′, hCAT-1 *anti*-sense: 5′-TGTTCACAATTAGCCCAGAG-3′, eNOS sense: 5′-CCAGCTAGCCAAAGTCACCAT-3′, eNOS *anti*-sense: 5′-GTCTCGGAGCCATACAGGATT-3′, IR-A sense: 5′-GCTGAAGCTGCCCTCGAGGA-3′, IR-A *anti*-sense: 5′-CGAGATGGCCTGGGGACGAA-3′, IR-B sense: 5′-GCTGAAGCTGCCCTCGAGGA-3′, IR-B *anti*-sense 5′-AGATGGCCTAGGGTCCTCGG-3′, 28S sense: 5′-TTGAAAATCCGGGGGAGAG-3′, 28S *anti*-sense: 5′-ACATTGTTCCAACATGCCAG-3′. Expected size products were hCAT-1 148 bp, eNOS 354 bp, IR-A 210 bp, IR-B 244 bp, and 28S 100 bp.

2.9. Intracellular NO determination

Intracellular NO was determined using the fluorescent dye DAF-FM. Confluent cells grown on 100 mm^2 culture plate were incubated in the absence or presence of insulin (1 nmol/L, 8 h) and exposed (45 min, 37 °C) to 10 μmol/L DAF-FM in PBS (37 °C, pH 7.4). The fluorescence ($\lambda_{exc}/\lambda_{em}$: 495/510 nm) was determined in a Sinergy 2 microplate reader (Biotek, Winooski, VT, USA) [17].

2.10. NOS activity

NOS activity was assayed by quantification of the intracellular content of L-citrulline by high performance liquid chromatography in confluent HUVECs in the absence or presence of 100 μmol/L L-NAME, as reported [17].

2.11. Human umbilical vein reactivity

Ring segments of 2-4 mm in length were dissected from human umbilical veins in ice-cold PBS (pH 7.4, 4 °C). Vein rings were mounted in a myograph (610M Multiwire Myograph System, Danish Myo Technology A/S, Denmark) for isometric force measurements in a Krebs physiological solution (mmol/L: 118.5 NaCl, 4.7 KCl, 25 $NaHCO_3$, 1.2 $MgSO_4$, 1.2 KH_2PO_4, 2.5 $CaCl_2$, 5.5 D-glucose, 0.3 L-arginine, 37 °C, pH 7.4). Vein rings were constantly bubbled with a mixture of 95% O_2/5% CO_2. The optimal diameter for each vessel was adjusted through the determination of the maximal active response evoked by 65 mmol/L KCl [13]. Endothelium-dependent relaxation was evaluated as the concentration-dependent response to CGRP (0.01 − 100 nmol/L, 5 min) and insulin (0.01 − 1000 nmol/L, 5 min) in KCl-preconstricted vessels. Experiments were performed in the absence or presence of 100 μmol/L L-NAME. Changes in isometric tension were recorded using the software LabChart (LabChart 7 for Windows, ADInstruments, Australia) coupled to a PowerLab (PowerLab 8/30 Data Acquisition System, ADInstruments, Australia).

2.12. Statistical analysis

The sample size was estimated considering a power of 80% to detect a difference between groups (on the basis of a two-sided alpha level of 0.05). Values for clinical parameters are given as mean ± S.D. For *in vitro* assays the values were mean ± S.E.M., where *n* indicates number of different biological samples and corresponding cell cultures with 3–4

Table 1
Clinical characteristics of pregnant women and newborns.

Variable	Normal (n = 13)	GDM*d* (n = 14)	GDM*i* (n = 18)
Mother			
Age (years)	32.1 ± 3.8	33.7 ± 5.2	30.5 ± 4.5
Height (cm)	162.5 ± 4.3	157.6 ± 6.1	160.2 ± 4.4
Weight (kg)			
Pre-pregnancy	62.8 ± 7.7	69.2 ± 9.3	72.2 ± 10.9*
1st trimester	63.3 ± 8.2	70.1 ± 9.6	72.5 ± 10.8*
2st trimester	67.4 ± 6.2	74.3 ± 7.9	79.2 ± 9.5*
3th trimester	73.7 ± 4.6	76.1 ± 8.8	81.0 ± 10.6
Term	73.8 ± 4.9	78.1 ± 4.1	82.1 ± 9.4*
BMI (kg/m^2)			
Pre-pregnancy	23.8 ± 2.5	26.9 ± 3.2	28.3 ± 3.9*
1st trimester	23.6 ± 2.7	27.8 ± 3.2*	28.4 ± 4.1*
2nd trimester	25.4 ± 1.9	28.9 ± 3.1*	31.1 ± 2.9*
3th trimester	28.1 ± 0.8	33.1 ± 2.8*	31.4 ± 3.6*
Term	28.1 ± 1.4	33.4 ± 4.4*	32.5 ± 3.1*
Systolic blood pressure (mm Hg)			
Pre-pregnancy	101.4 ± 6.9	113.9 ± 9.9	104.6 ± 6.3
1st trimester	106.9 ± 5.4	110.1 ± 11.1	106.7 ± 7.7
2nd trimester	105.7 ± 9.8	109.2 ± 9.2	105.4 ± 9.7
3th trimester	108.1 ± 7.5	109.6 ± 15.6	109.5 ± 11.7
Term	113.8 ± 5.2	110.4 ± 7.1	110.2 ± 10.6
Diastolic blood pressure (mm Hg)			
Pre-pregnancy	62.9 ± 4.9	70.7 ± 6.2	68.6 ± 6.3
1st trimester	67.7 ± 6.4	65.2 ± 9.1	66.4 ± 6.1
2nd trimester	67.1 ± 7.6	66.3 ± 8.5	65.7 ± 5.8
3th trimester	66.3 ± 5.8	69.2 ± 10.1	69.5 ± 7.7
Term	67.5 ± 8.9	72.2 ± 8.8	71.5 ± 5.1
Mean arterial pressure (mm Hg)			
Pre-pregnancy	75.7 ± 4.6	70.7 ± 6.2	80.6 ± 5.2
1st trimester	80.8 ± 3.9	81.8 ± 8.6	80.1 ± 5.6
2nd trimester	80.1 ± 7.2	81.9 ± 9.2	78.9 ± 6.7
3th trimester	80.2 ± 6.2	82.7 ± 11.8	82.8 ± 8.2
Term	82.9 ± 7.1	84.3 ± 7.1	84.4 ± 5.7
Glycemia fasting (mg/dL)	82.9 ± 7.1	85.1 ± 4.9	87.8 ± 8.1
OGTT (mg/dL)			
Glycemia basal	78.3 ± 5.1	85.8 ± 8.8	84.4 ± 15.3
Glycemia 2 h after glucose	82.9 ± 7.1	155.5 ± 13.9*	165.9 ± 20.1*
Newborn			
Sex (female/male)	7/6	8/6	10/8
Gestational age (weeks)	38.5 ± 1.3	38.8 ± 0.6	38.4 ± 0.6
Birth weight (grams)	3374 ± 411	3441 ± 447	3552 ± 517
Height (cm)	50.2 ± 1.3	50.1 ± 1.5	50.1 ± 1.4
Ponderal index (grams/cm^3 × 100)	2.7 ± 0.3	2.7 ± 0.2	2.8 ± 0.3

Women that coursed with normal pregnancies (*Normal*), GDM under treatment with diet (GDM*d*) or GDM*d* passed onto insulin therapy (GDM*i*) were included in this study. Weight, body mass index (BMI), and blood pressure were determined before pregnancy (pre-pregnancy) and at 1st (0–14 weeks of gestation (wg)), 2nd (14–28 wg) or 3th (28–40 wg) trimesters of pregnancy and at term (38–41 wg). Values for pre-pregnancy weight and blood pressure correspond to those autoreferred by patients. In Normal pregnancies, 11 women were with pre-pregnancy normal weight (BMI < 25 kg/m^2) and two with pre-pregnancy overweight (BMI ≥ 25 and < 30 kg/m^2). In GDM*d*, 11 women were with pre-pregnancy normal weight, two pre-pregnancy overweight, and one pre-pregnancy obese (BMI ≥ 30 kg/m^2). In GDM*i*, 14 women were with pre-pregnancy normal weight, two pre-pregnancy overweight, and two pre-pregnancy obese. BMI was calculated by weight in kilograms divided by the square of the height in meters. Ponderal index was calculated by weight in grams divided by the cube of height in centimeters multiplied by 100. Oral glucose tolerance test (OGTT) was measured at 24–28 weeks of gestation in all women with a normal glycaemia (see Material and methods).
Values are mean ± S.D.
* $P < 0.05$ versus corresponding values in *Normal*.

replicates per experiment. Comparisons between two groups were performed by means of Student's unpaired *t*-test and between more than two groups by analysis of variance (ANOVA, two-ways). If the ANOVA demonstrated a significant interaction between variables, *post hoc* analyses were performed by the multiple-comparison Bonferroni test. The statistical software GraphPad InStat 3.1 and GraphPad Prism 7.0c (GraphPad Software Inc., San Diego, CA, USA) was used for data analysis. $P < 0.05$ was considered statistically significant.

3. Results

3.1. Study groups

Pregnancies were singleton, and pregnant women showed with similar age and height, were normotensive, and with normal fasting glycaemia at term (Table 1). The total gestational weight gain between pre-pregnancy and term was 10 ± 1 kg in normal pregnancies, 8.9 ± 0.9 kg in GDM*d* pregnancies, and 9.9 ± 1.1 kg in GDM*i* pregnancies. Clinical parameters of newborns from the three study groups did not show significant differences.

3.2. L-Arginine transport kinetics

The v_i for overall 100 μmol/L L-arginine transport was lineal up to 60 s in cells from normal, GDM*d*, or GDM*i* pregnancies without insulin (Fig. 1A). Values for v_i were higher in cells from GDM*d* and GDM*i* compared with normal pregnancies (Table 2). Overall L-arginine transport was semisaturable in cells without insulin from normal, GDM*d*, or GDM*i* pregnancies (Fig. 1B), with K_D values higher in GDM*d* and GDM*i* compared with normal pregnancies (Table 2). After substracting the lineal, non-saturable transport component from overall transport, the remaining L-arginine transport was saturable, best fitted by a single Michaelis-Menten equation (Fig. 1C), and lineal in an Eadie-Hofstee plot (Fig. 1D). Saturable transport showed with higher V_{max} in cells from GDM*d* and GDM*i* compared with normal pregnancies. The apparent K_m values were not significantly altered in cells from these three study groups. However, the maximal transport capacity (V_{max}/K_m) was higher in GDM*d* and GDM*i* when compared with normal pregnancies (Table 2).

Insulin increased the v_i and K_D in cells from normal pregnancies, but restored this parameter in GDM*d* and GDM*i* (Fig. 1E). Overall transport in the presence of insulin was also semisaturable (Fig. 1F), and saturable transport showed higher V_{max} and V_{max}/K_m, but unaltered K_m values in cells from normal pregnancies (Fig. 1G). GDM*d* and GDM*i*-increased L-arginine transport was blocked by insulin. Eadie-Hofstee plot of saturable data was lineal in cells treated with insulin from all study groups (Fig. 1H).

3.3. hCAT-1 protein abundance and mRNA expression

In cells without insulin the hCAT-1 protein abundance was higher in GDM*d* and GDM*i* compared with normal pregnancies (Fig. 2A). Incubation of cells with insulin, increased hCAT-1 protein abundance in normal pregnancies, but partially reduced its abundance in GDM*d* and GDM*i*. Similar results were obtained for hCAT-1 mRNA expression without or with insulin; however, insulin fully reversed GDM*d* effect (Fig. 2B).

3.4. Involvement of p44/42^{mapk} and Akt on L-arginine transport

Cells from GDM*d* and GDM*i* without insulin show increased p44/42^{mapk} phosphorylation compared with normal pregnancies (Fig. 3A). Insulin blocked the GDM*d* and GDM*i* effect, but increased p44/p42^{mapk} phosphorylation in cells from normal pregnancies. Phosphorylated Akt protein abundance was unaltered by GDM*d* or GDM*i*, or insulin in cells from normal or GDM pregnancies. IR-A mRNA expression was higher in cells from GDM*d* and GDM*i* compared with normal pregnancies (Fig. 3B). Insulin blocked GDM effect on IR-A mRNA expression, but unaltered its expression in cells from normal pregnancies. However, IR-B mRNA expression was unaltered by GDM or insulin.

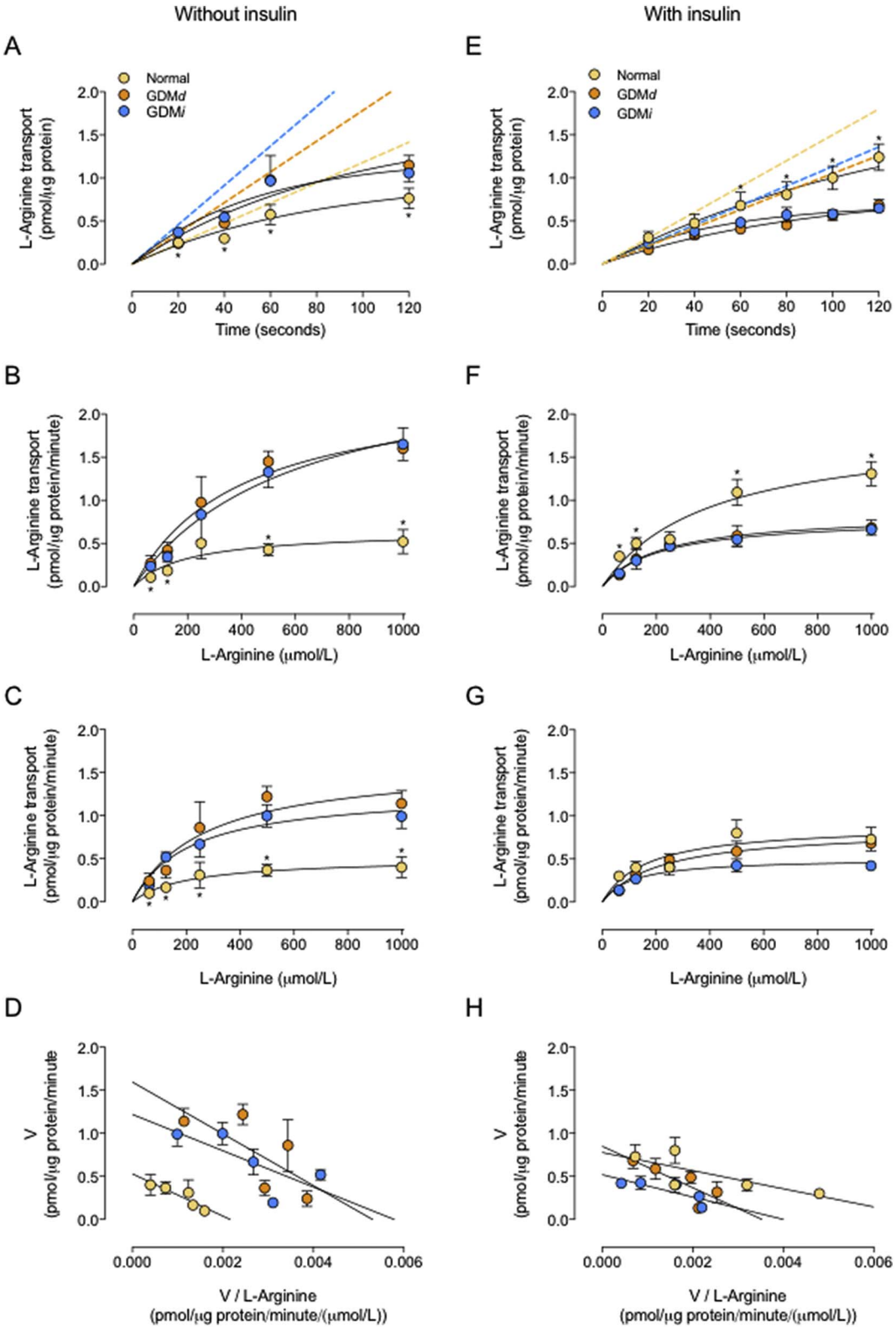

Fig. 1. L-Arginine transport in HUVECs from GDM*i* pregnancies. A. Initial velocity of 100 µmol/L L-arginine uptake at various times in HUVECs from normal, gestational diabetes on diet (GMD*d*), and GDM*d* into insulin therapy (GDM*i*) without exogenous insulin *in vitro*. Straight dashed lines represent the lineal phase of uptake estimated for 0.5 s incubation (see Material and methods). B. Overall L-arginine transport measured at initial velocity fitted to a single Michaelis-Menten equation increased in a lineal component (see Material and methods). C. Saturable L-arginine transport derived from data in B adjusted to a single Michaelis-Menten equation. D. Eadie-Hofstee representation of data in C. E to H are cells in the presence (8 h) of 1 nmol/L insulin (with insulin). *$P < 0.05$ versus corresponding values in GDM*i* or GDM*d*. For some data points the error bars were smaller than the symbols. Values are mean ± S.E.M. ($n = 7$–11).

Table 2
Kinetic parameters for L-arginine transport in HUVECs from normal or GDM pregnancies.

	Saturable transport			Overall transport	
	V_{max} (pmol/μg protein/minute)	K_m (μmol/L)	V_{max}/K_m (pmol/μg protein/minute/(μmol/L))	K_D (pmol/μg protein/minute/(μmol/L))	v_i (pmol/μg protein/0.5 s)
Normal pregnancies (n = 13)					
Without insulin					
Control	0.50 ± 0.06	144 ± 55	0.0035 ± 0.0009	0.00012 ± 0.0001	0.00171 ± 0.00021
PD-98059	0.60 ± 0.07	197 ± 59	0.0030 ± 0.0006	0.00014 ± 0.0001	0.00168 ± 0.00017
Inh-IV	0.45 ± 0.07	123 ± 71	0.0037 ± 0.0013	0.00015 ± 0.0003	0.00168 ± 0.00031
PD-98059 + Inh-IV	0.53 ± 0.05	274 ± 58	0.0019 ± 0.0003	0.00012 ± 0.0001	0.00118 ± 0.00009
With insulin					
Control	0.89 ± 0.07*	164 ± 42	0.0054 ± 0.0009*	0.00044 ± 0.0001*	0.00281 ± 0.00023*
PD-98059	0.62 ± 0.09**	223 ± 90	0.0028 ± 0.0008**	0.00012 ± 0.0001**	0.00159 ± 0.00021**
Inh-IV	0.63 ± 0.03**	123 ± 15	0.0051 ± 0.0004*	0.00040 ± 0.0001*	0.00235 ± 0.00010*
PD-98059 + Inh-IV	0.46 ± 0.03**	258 ± 40	0.0030 ± 0.0009**	0.00024 ± 0.0001**	0.00107 ± 0.00005**
GDM*d* pregnancies (n = 14)					
Without insulin					
Control	1.61 ± 0.14*	269 ± 61	0.0060 ± 0.0009*	0.00046 ± 0.0001*	0.00363 ± 0.00028*
PD-98059	0.65 ± 0.07**	143 ± 51	0.0045 ± 0.0010**	0.00092 ± 0.0003*,***	0.00223 ± 0.00025**
Inh-IV	1.44 ± 0.20*	295 ± 96	0.0049 ± 0.0012*	0.00040 ± 0.0001*	0.00303 ± 0.00035*
PD-98059 + Inh-IV	0.93 ± 0.09**	211 ± 53	0.0044 ± 0.0005**	0.00080 ± 0.0002*,***	0.00249 ± 0.00021**
With insulin					
Control	0.61 ± 0.03***	141 ± 24	0.0042 ± 0.0005‡	0.00019 ± 0.0001‡	0.00210 ± 0.00028‡
PD-98059	0.83 ± 0.04***	210 ± 27	0.0039 ± 0.0004***	0.00096 ± 0.0001*,***	0.00227 ± 0.00023***
Inh-IV	0.49 ± 0.03***	159 ± 23	0.0031 ± 0.0003***	0.00040 ± 0.0001*,***	0.00298 ± 0.00025*
PD-98059 + Inh-IV	0.73 ± 0.07***	144 ± 45	0.0051 ± 0.0010***	0.00114 ± 0.0003*,***	0.00208 ± 0.00026***
GDMi pregnancies (n = 18)					
Without insulin					
Control	1.28 ± 0.07*	213 ± 32	0.0060 ± 0.0006*	0.00066 ± 0.0003*	0.00340 ± 0.00017*
PD-98059	0.92 ± 0.14**	223 ± 75	0.0041 ± 0.0009**	0.00056 ± 0.0001*	0.00237 ± 0.00028**
Inh-IV	1.48 ± 0.09*	254 ± 40	0.0058 ± 0.0007*	0.00022 ± 0.0001*,***	0.00348 ± 0.00018*
PD-98059 + Inh-IV	0.63 ± 0.08**	164 ± 60	0.0038 ± 0.0009**	0.00102 ± 0.0010*,***	0.00198 ± 0.00024**
With insulin					
Control	0.51 ± 0.03***	111 ± 17	0.0046 ± 0.0005***	0.00024 ± 0.0003***	0.00201 ± 0.00010***
PD-98059	0.46 ± 0.03***	108 ± 24	0.0043 ± 0.0006***	0.00120 ± 0.0010*,***	0.00184 ± 0.00013***
Inh-IV	0.54 ± 0.03***	193 ± 29	0.0028 ± 0.0003‡	0.00036 ± 0.0001*,***	0.00153 ± 0.00007***
PD-98059 + Inh-IV	0.62 ± 0.09***	218 ± 93	0.0028 ± 0.0014***	0.00130 ± 0.0010*,***	0.00162 ± 0.00023***

L-Arginine transport (0–1000 μmo/L, 1 min, 37 °C) was measured in HUVECs from normal pregnancies (Normal), GDM under treatment with diet (GDM*d*) or GDM*d* passed onto insulin therapy (GDM*i*) exposed (8 h) to culture medium without (*Without insulin*) or with (*With insulin*) insulin (1 nmol/L). Transport assays were done in the absence (Control) or presence of the PD- 98059 (10 μmol/L, MEK1/2 inhibitor) and Akt Inhibitor IV (Inh-IV, 1 μmol/L) or both (see Material and methods). Maximal velocity (V_{max}) and apparent Michaelis-Menten constant (K_m) of saturable transport were calculated assuming a single Michaelis-Menten hyperbola. V_{max}/K_m represents maximal L-arginine transport capacity. The lineal phase of overall transport of L-arginine (K_D) was obtained from transport data fitted to a Michaelis-Menten equation increased in a lineal component. Initial velocity (v_i) was calculated for 0.5 s with 100 μmol/L L-arginine transport.
Values are mean ± S.E.M.
* $P < 0.05$ versus corresponding Control values in Normal *Without insulin*.
** $P < 0.05$ versus corresponding Control values.
*** $P < 0.05$ versus corresponding Control values *Without insulin*.

Overall L-arginine transport in the presence of PD-98059 and Inh-IV was semisaturable as in the absence of these inhibitors (not shown). Incubation of cells with PD-98059, Inh-IV, or both, did not alter the v_i or K_D values in cells from normal pregnancies without insulin (Table 2). However, insulin-stimulatory effect on these parameters was blocked by PD-98059 or PD-98059 + Inh-IV, but unaltered by Inh-IV alone. Insulin-increased V_{max} and V_{max}/K_m for saturable transport was blocked by PD-98059 or PD-98059 + Inh-IV; however, Inh-IV alone blocked the increase caused by insulin in the V_{max}/K_m, but not in V_{max} (Fig. 3C, Table 2). In cells without insulin the GDM*d*-increased v_i and V_{max} were blocked only by PD-98059 or PD-98059 + Inh-IV. The GDM*d*-increased V_{max}/K_m was blocked by PD-98059, Inh-IV, or PD-98059 + Inh-IV. However, incubation of cells with PD-98059 or PD-98059 + Inh-IV, but not with Inh-IV alone, resulted in higher K_D values compared with cells from GDM*d* in the absence of these inhibitors (Table 2). Insulin reversed the increase caused by GDM*d* in all the kinetic parameters in the absence or presence of inhibitors. However, K_D values in cells with insulin and inhibitors were unaltered compared with cells without insulin in the presence of the inhibitors. The inhibitors caused a similar pattern of inhibition in cells from GDM*i* without insulin, except for cells incubated with PD-98059 where K_D value was unaltered compared with cells in the absence of this inhibitor (Table 2). In cells with insulin the pattern of effects of the inhibitors in the kinetic parameters was similar compared to those in cells from GDM*d*, except for Inh-IV which inhibits the increase in v_i caused by GDM*i*.

3.5. NOS activity

The intracellular content of L-citrulline generated by NOS activity (i.e., fraction inhibited by L-NAME) was higher reaching similar values in cells from GDM*i* and GDM*d*, compared with normal pregnancies (Fig. 4A). Insulin caused a substantial reduction in GDM-increased L-citrulline content, but increased intracellular content of this amino acid in cells from normal pregnancies. In addition, the NO level detected in cells from GDM*d* and GDM*i* was higher than normal pregnancies (Fig. 4B). Insulin increased NO level in cells from normal pregnancies, and partially reversed the effect of GDM.

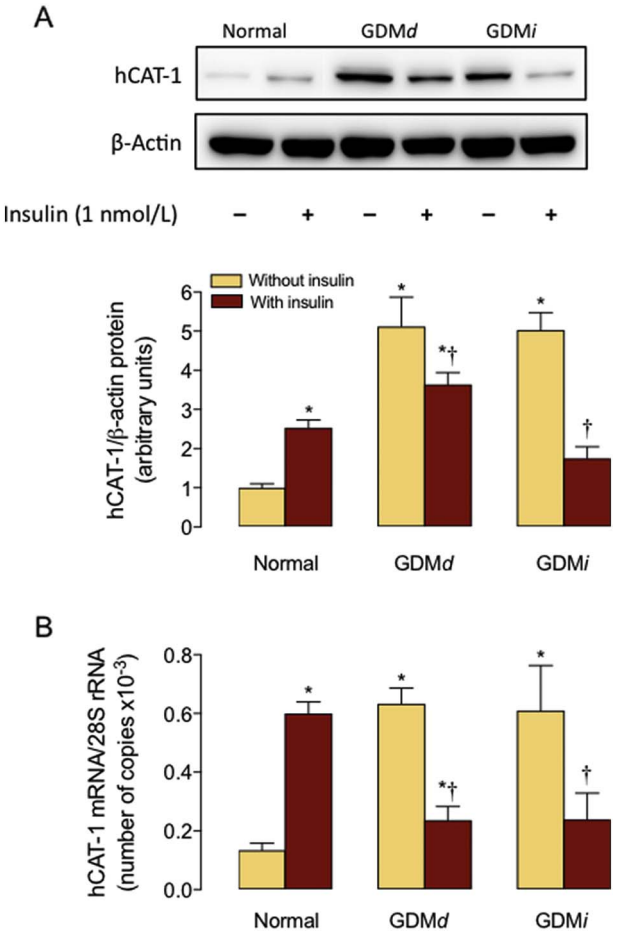

Fig. 2. hCAT-1 expression in HUVECs from GDM*i* pregnancies. A. Western blot for hCAT-1 and β-actin (internal reference) protein abundance in HUVECs from normal, gestational diabetes on diet (GMD*d*), and GDM*d* into insulin therapy (GDM*i*) without or with (8 h) exogenous insulin *in vitro*. *Lower panel*: hCAT-1/β-actin ratio densitometries normalized to 1 in Normal. B. hCAT-1 mRNA expression as in A. $^{*}P < 0.05$ versus Normal Without insulin. $^{\dagger}P < 0.05$ versus corresponding values Without insulin. Values are mean ± S.E.M. ($n = 5$).

3.6. eNOS expression and phosphorylation

Cells from GDM*d* and GDM*i* without insulin show comparable higher eNOS protein abundance compared with normal pregnancies (Fig. 4C). Insulin partially reduced GDM effect on eNOS, but increased its protein abundance in cells from normal pregnancies. In cells without insulin the P-Ser^{1177} eNOS protein abundance was higher in GDM pregnancies reaching similar values, an effect blocked by insulin in cells from GDM*d*, but partially reversed by this hormone in GDM*i* (Fig. 4D). Insulin increased P-Ser^{1177} eNOS protein abundance in cells from normal pregnancies. However, neither GDM nor insulin altered P-Thr^{496} eNOS protein abundance (Fig. 4E). GDM*d* and GDM*i* associated with higher and comparable eNOS mRNA expression (Fig. 4F) compared with cells from normal pregnancies. Insulin reversed the GDM effect on eNOS mRNA, but increased mRNA expression in cells from normal pregnancies.

3.7. Umbilical vein reactivity

Insulin caused concentration, NOS-dependent relaxation in umbilical vein rings (Fig. 5A). Maximal relaxation (R_{max}) in response to insulin was lower, but half-maximal effect (EC_{50}) was higher in vein rings from GDM*d* and GDM*i* compared with normal pregnancies (Table 3). The required insulin concentration to cause a similar R_{max} (i.e., EC_{50}/R_{max}) was higher in GDM*d* and GDM*i* compared with normal pregnancies. The EC_{50}/R_{max} was higher in GDM*i* compared with vessel rings from GDM*d*. CGRP also caused concentration-dependent relaxation of vein rings (Fig. 5B) with an EC_{50} values lower than those for insulin effect in vessel rings from all conditions (Table 3). The EC_{50} in vein rings from GDM*d* was lower than vessel rings from normal or GDM*i* pregnancies, but higher in samples from GDM*i* (Table 3). The R_{max} in response to CGRP was similar than in response to insulin in normal pregnancies. The EC_{50}/R_{max} values for CGRP were higher in GDM*d* and GDM*i* compared with normal pregnancies, higher in GDM*i* compared with GDM*d* pregnancies. In addition, the EC_{50}/R_{max} values for CGRP were higher for vessel rings from all pregnancies.

4. Discussion

This study shows for the first time that HUVECs from pregnancies where the mother with GDM*d* was subjected to insulin therapy (GDM*i*) exhibit increased L-arginine transport and NO synthesis, which was comparable to cells from GDM*d* without insulin therapy or from normal pregnancies exposed to insulin *in vitro*. Cells from GDM*i* show increased p44/42^{mapk} activation and IR-A mRNA expressiom, but unaltered Akt activation and IR-B expression. Insulin *in vitro* reversed GDM*i* effect on L-arginine transport, NO synthesis and p44/42^{mapk} activation. NO and endothelium-dependent dilation of umbilical vein rings from GDM*i* was reduced in response to insulin compared with GDM*d* or normal pregnancies. Mothers and newborns from GDM*i* showed with normoglycaemia at term, but insulin therapy seems not enough to restore associated foetoplacental vascular dysfunction.

GDM associates with reduced foetoplacental vascular reactivity due to microvascular [26] and macrovascular [12,13,16] endothelial dysfunction [5,6]. HUVECs from women with GDM*d* (i.e., without insulin therapy) show increased L-arginine transport mediated by hCAT-1 [13] and NO synthesis due to eNOS activation [16] compared with normal pregnancies. Incubation of HUVECs from GDM*d* with insulin *in vitro* reversed the increased transport of L-arginine (half-maximal effective dose (ED_{50}) ~0.3 nmol/L) [27] and NO synthesis (ED_{50} ~0.4 nmol/L) [12] seen in this condition. Our results show that HUVECs from GDM*i* pregnancies exhibit similar changes to those in GDM*d* pregnancies. Thus, insulin therapy does not restores GDM*d*-associated human umbilical vein endothelial dysfunction. L-Arginine transport is mainly mediated by hCAT-1 with an apparent K_m ~100–200 μmol/L in HUVECs from normal pregnancies [28–30], a value close to the concentration of this amino acid in the human umbilical vein blood (~80 μmol/L) [31,32]. Thus, hCAT-1 plays a crucial role in the uptake of L-arginine in HUVECs. Saturable L-arginine transport in HUVECs from GDM*i*, and GDM*d* pregnancies shows apparent K_m within hCAT-1 range. Furthermore, hCAT-1 protein and mRNA expression were higher in HUVECs from GDM*i* and GDM*d* compared with normal pregnancies. Thus, hCAT-1 is likely involved in the removal of L-arginine from the extracellular medium, and GDM*i* or GDM*d* unaltered this membrane transporter's intrinsic properties. hCAT-2B, another member of hCATs family [14,15], is coexpressed with hCAT-1 in HUVECs [33] mediating L-arginine transport with K_m ~300–400 μmol/L [14,15]. Therefore, hCAT-2B may also mediate L-arginine transport in HUVECs from GDM*i* pregnancies. However, since Eadie-Hofstee plot of saturable transport and overall transport up to 250 μmol/L L-arginine were lineal, it is likely that a single membrane transport system in the range of 100–200 μmol/L (likely hCAT-1), or more than one transport system with K_m within this range, accounted for uptake of L-arginine into HUVECs. hCAT-1 involvement on GDM*i* and GDM*d*-increased transport is further supported by the results showing that hCAT-1 protein abundance and mRNA expression was higher (~5 fold) in cells from GDM*i* and GDM*d* compared with normal pregnancies. Thus, increased L-arginine transport may result from higher hCAT-1 availability in HUVECs. Since the V_{max} increase in GDM*i* and GDM*d* versus normal pregnancies was ~2.6 and ~3.2 fold, respectively, and because these conditions

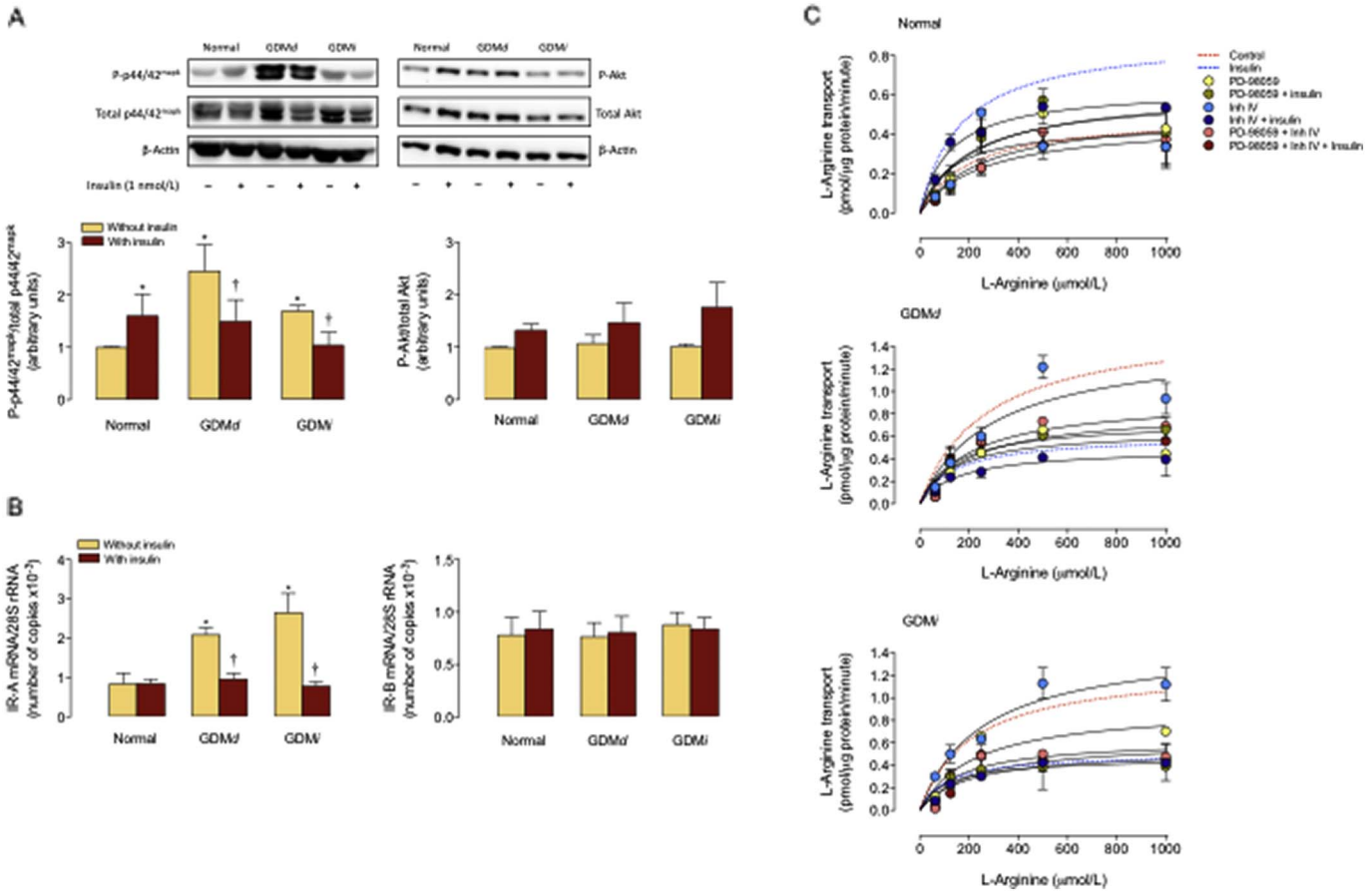

Fig. 3. Involvement of p44/42^{mapk} and Akt on L-arginine transport in HUVECs from GDM*i* pregnancies. A. Western blot for total (Total p44/42^{mapk}) and phosphorylated (P-p44/42^{mapk}) p44/42^{mapk}, and total (Total Akt) and phosphorylated (P-Akt) Akt, and β-actin (internal reference) protein abundance in HUVECs from normal, gestational diabetes on diet (GMD*d*), and GDM*d* into insulin therapy (GDM*i*) without or with (8 h) exogenous insulin *in vitro*. *Lower panels*: P-p44/42^{mapk}/total p44/42^{mapk} or P-Akt/total Akt ratio densitometries normalized to 1 in Normal Without insulin. B. Insulin receptor A (IR-A) and B (IR-B) mRNA expression in HUVECs as in A. C. Saturable L-arginine transport measured at initial velocity adjusted to a single Michaelis-Menten equation in cells incubated in the presence of PD-98059 (10 µmol/L), Akt Inhibitor IV (Inh-IV, 1 µmol/L), or both, without or with insulin (1 nmol/L). Saturable L-arginine transport in cells in the absence of insulin and inhibitors (Controls, red dotted lines) or presence of insulin (Insulin, 1 nmol/L, blue dotted lines) from Fig. 1C and G are shown. $^{*}P < 0.05$ versus Normal Without insulin. †$P < 0.05$ versus corresponding values Without insulin. Values are mean ± S.E.M. ($n = 5$).

caused similar increase in hCAT-1 expression, a fraction not larger than 36–50% may be due to a change in hCAT-1 expression or availability at the plasma membrane in HUVECs from GDM*i* and GDM*d*.

The V_{max} and V_{max}/K_m values in GDM*i* were similar to those in GDM*d* pregnancies, but higher compared with normal pregnancies. Thus, insulin therapy does not result in reversal of hCAT-1–mediated maximal transport capacity in HUVECs from GDM pregnancies. Since the increase in V_{max}/K_m was similar in GDM*i* and GDM*d*, but GDM*i* caused lower increase in V_{max} compared with GDM*d* ($^{GDMi}V_{max}/^{GDMd}V_{max} \sim 0.7$), different component(s) to those in GDM*d* may modulate L-arginine transport in cells from GDM*i* pregnancies. Interestingly, overall L-arginine transport for values > 250 µmol/L showed higher K_D for GDM*i* compared with GDM*d* (~1.43 fold) and normal pregnancies (~5.5 fold). Thus, along with hCAT-1, L-arginine uptake seems mediated via a transport system(s) that does not gets saturated up to 1000 µmol/L in cells from GDM*i* and GDM*d* pregnancies. Since apparent K_m for hCAT-3, member of hCATs family [14,15], is > 500 µmol/L [34], these transporters may be involved in overall L-arginine transport playing a minor contribution at < 250 µmol/L L-arginine in HUVECs.

Phosphorylation of p44/42^{mapk} was increased, but Akt phosphorylation was unaltered in cells from GDM*i* compared with normal pregnancies or in HUVECs from women with GDM not separated by diet only versus diet plus insulin therapy (GDM*pool*) [28]. Since GDM*i* and GDM*d*-increased L-arginine transport was reversed by inhibiting p44/42^{mapk}, but unaltered by Akt inhibition, increased transport may result from p44/42^{mapk} activation. This is likely in cells from GDM*i*, but may only partially explain the GDM*d* increase in transport (increased p44/42^{mapk} phosphorylation/increased transport ~0.53). It is likely that increased IR-A expression accounts for GDM*i* effects since activation or overexpression of this type of insulin receptors results in preferential activation of p44/42^{mapk} (i.e., p44/42^{mapk} activation/Akt activation > 1) in HUVECs [5,12,16]. All together these findings highlight potential differences on L-arginine transport modulation in HUVECs from these two conditions of pregnancy. Previous studies show increased eNOS activity in HUVECs from GDM*pool* [28,35] or GDM*d* [16] pregnancies compared with normal pregnancies. We extended these observations to GDM*i* pregnancies where higher NO level and NOS activity was found, a phenomenon likely due to higher activator Ser^{1177} phosphorylation of eNOS [36,37]. Since eNOS protein abundance and mRNA expression were also increased in cells from these conditions, increased eNOS expression, reduced degradation or increased stability of eNOS protein or mRNA are alternative mechanisms that may be involved in this phenomenon.

Insulin restored the V_{max}/K_m of transport by reducing the V_{max} in cells from GDM*i* to values in normal pregnancies, confirming previous results in cells from GDM*pool* [28] or GDM*d* [13] pregnancies. Since the K_m was not changed by insulin, it is likely hCAT-1 affinity for L-arginine uptake is unaltered by this hormone in cells from GDM*i* pregnancies. However, since GDM*i*-increased K_D and v_i was reversed by insulin, this hormone may restore the functionality of an alternative mechanism, potentially hCAT-3, for L-arginine transport. Since insulin also restored

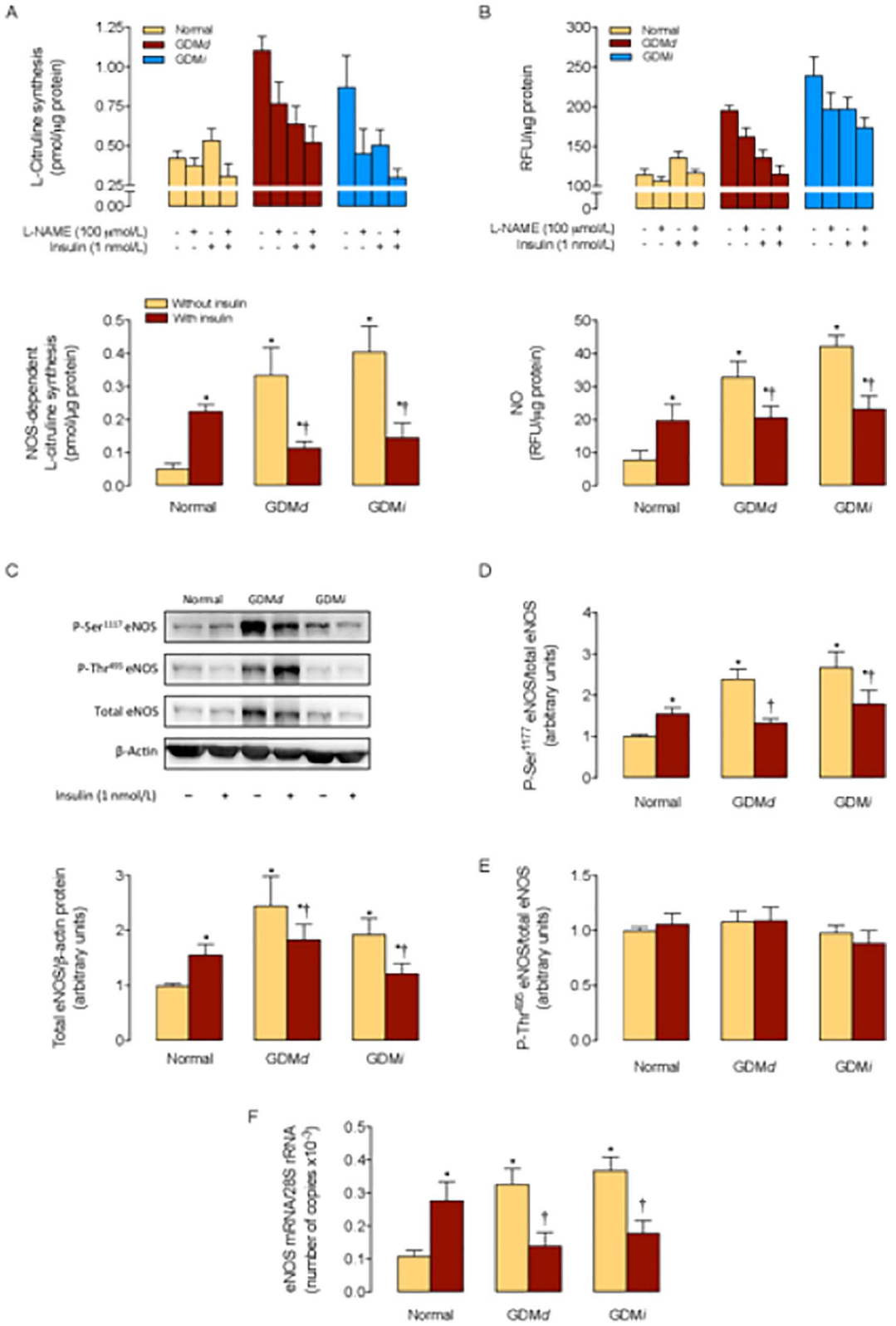

Fig. 4. Nitric oxide synthesis in HUVECs from GDM*i* pregnancies. A. L-Citrulline synthesis was measured by h.p.l.c. (see Material and methods) in HUVECs from normal, gestational diabetes on diet (GMD*d*), and GDM*d* into insulin therapy (GDM*i*) incubated without or with exogenous insulin (1 nmol/L, 8 h) *in vitro* in the absence or presence of N^G-nitro-L-arginine methyl ester (L-NAME, 100 µmol/L). *Lower panel:* L-citrulline synthesis via nitric oxide synthase (NOS) activity derived from data in A. B. Relative fluorescence units (RFU) were measured in cells preloaded with the fluorescent dye 4-amino-5-methylamino-2′,7′-difluorescein (DAF-FM, 10 µmol/L) as in A. *Lower panel:* nitric oxide (NO) generation via NOS activity derived from data in B. C. Western blot for total eNOS (Total eNOS), eNOS phosphorylated at serine^{1177} (P-Ser^{1177}-eNOS) or threonine^{495} (P-Thr^{495}-eNOS) and β-actin (internal reference) protein abundance as in A. The graph shows Total eNOS/β-actin ratio densitometries normalized to 1 in Normal Without insulin. D. P-Ser^{1177}-eNOS/total eNOS ratio densitometries normalized to 1 in Normal Without insulin from data in C. E. P-Thr^{495}-eNOS/total eNOS ratio densitometries normalized to 1 in Normal Without insulin from data in C. F. eNOS mRNA expression as in A. *$P < 0.05$ versus Normal Without insulin. †$P < 0.05$ versus corresponding values Without insulin. Values are mean ± S.E.M. ($n = 5$).

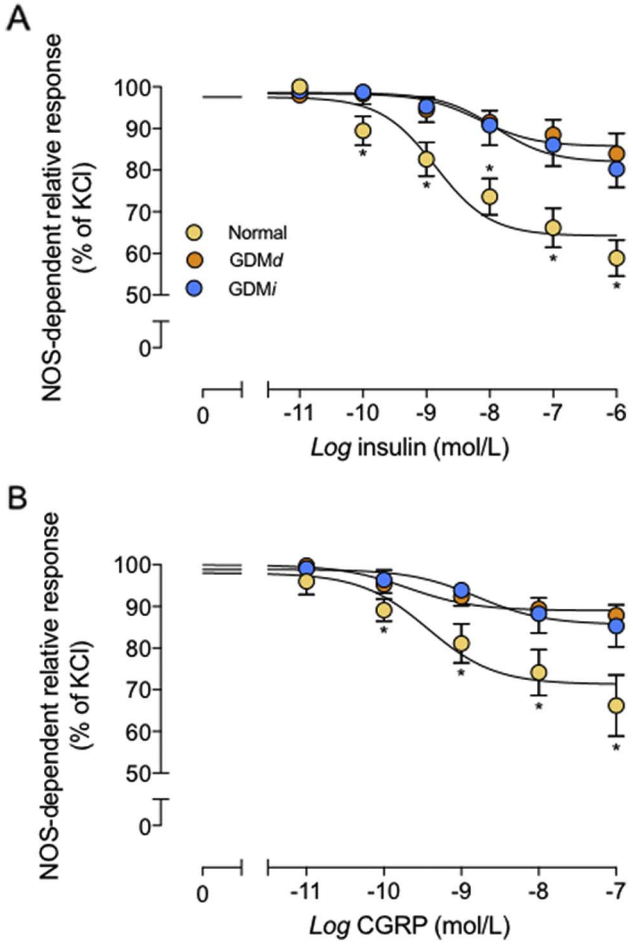

Fig. 5. Human umbilical vein dilation in GDM*i* pregnancies. A. Human umbilical vein rings isolated from normal, gestational diabetes on diet (GMD*d*), and GDM*d* into insulin therapy (GDM*i*) were incubated without (0) or with exogenous insulin in the absence or presence of N^G-nitro-L-arginine methyl ester (L-NAME, 100 μmol/L). B. Vein rings response to calcitonin gene related protein (CGRP) as in A. *$P < 0.05$ versus corresponding values in GDM*i* or GDM*d*. Values are mean ± S.E.M. (n = 3–6).

GDM*i*-increased hCAT-1 expression, this hormone may regulate hCAT-1 bioavailability in HUVECs from GDM*i* pregnancies. The contribution of a reduced hCAT-1 protein abundance to the lower V_{max}/K_m for transport caused by insulin in GDM*i* is partial since not more than two-thirds reduction in transport could be explained by changes in hCAT-1 protein abundance [(reduced V_{max}/K_m) / (reduced hCAT-1) − 1 is ~0.65]. However, in GDM*d* the reduced V_{max}/K_m could be explained by similar reduction in hCAT-1 protein abundance. Insulin-reduced hCAT-1 mRNA expression (~60%) was similar to this transporter's protein abundance in GDM*i* pregnancies. Since insulin-restoration of GDM*d*-increased hCAT-1 mediated transport in HUVECs resulted from lower protein abundance due to lower transcription of *SLC7A1* gene (for hCAT-1) [13], insulin restoration of GDM*i*-increased hCAT-1 mediated transport may result from a similar phenomenon.

Inhibition of $p44/42^{mapk}$ restores GDM*i*- and GDM*d*-increased L-arginine transport in the same proportion as insulin. Thus, $p44/42^{mapk}$ over-activation could be responsible for these pathological conditions's associated increased transport, complementing similar results in cells from normal pregnancies in response to insulin [28,33]. Insulin also activates insulin receptor A (IR-A) that mediates preferential activation of $p44/42^{mapk}$ compared with Akt ($p44/42^{mapk}$/Akt > 1), and insulin receptor B (IR-B) mediating preferential Akt activation compared with $p44/42^{mapk}$ ($p44/42^{mapk}$/Akt < 1) in HUVECs [16]. Since HUVECs from GDM*i* in the absence of exogenous insulin show $p44/42^{mapk}$/Akt ~1.7, a value close to the increase in V_{max}/K_m, IR-A signalling is likely

Table 3
Vasodilation parameters in human umbilical vein rings.

	Normal (n = 13)	GDM*d* (n = 14)	GDM*i* (n = 18)
Insulin			
EC_{50} (nmol/L)	1.39 ± 0.05	6.95 ± 0.31*	12.3 ± 0.71***
R_{max} (%)	38 ± 6	14 ± 2*	18 ± 3*
EC_{50}/R_{max} (a.u.)	0.037 ± 0.005	0.496 ± 0.005*	0.682 ± 0.007***
CGRP			
EC_{50} (nmol/L)	0.37 ± 0.02***	0.20 ± 0.03****	1.62 ± 0.31*****
R_{max} (%)	29 ± 5	12 ± 4*	14 ± 3*
EC_{50}/R_{max} (a.u.)	0.013 ± 0.001***	0.017 ± 0.003****	0.121 ± 0.002*****

Human umbilical vein rings were obtained from cords from normal pregnancies (Normal), GDM under treatment with diet (GDM*d*) or GDM*d* passed onto insulin therapy (GDM*i*). Vein rings were preconstricted with 65 mmol/L KCl and incubated with increasing concentrations of insulin (0.01–1000 nmol/L) or calcitonin gene related protein (CGRP) (0.01–100 nmol/L) in the absence or presence of N^G-nitro-L-arginine methyl ester (L-NAME, 100 μmol/L). Half-maximal effective concentration (EC_{50}) and maximal relaxation (R_{max}) were calculated for the difference in insulin and CGRP response in the absence or presence of L-NAME (i.e., nitric oxide synthase (NOS)-dependent relative response).
Values are mean ± S.E.M.
a.u., arbitrary units.
* $P < 0.05$ versus corresponding values in Normal.
** $P < 0.05$ versus corresponding values in GDM*d*.
*** $P < 0.05$ versus corresponding values in the presence of *Insulin*.

increased in GDM*i*. Indeed, IR-A, but not IR-B mRNA expression is higher in cells from GDM*i* compared with normal pregnancies, and is similar to the increase seen in GDM*d*, as reported [12,16]. Since insulin restored $p44/42^{mapk}$/Akt in cells from GDM*i*, and GDM*i*-increased IR-A mRNA is reversed to values in normal pregnancies, insulin beneficial effect on L-arginine transport, NO synthesis and eNOS expression and activation in HUVECs from GDM*i* was likely due to restoring IR-A expression and its associated cell signalling. A likely functional consequence of the described alterations caused by GDM at a cellular level, is a lower response of umbilical vessels to insulin. The results show that required insulin to generate a NO-dependent dilation of these vessels [($^{Normal}EC_{50}/R_{max}$) / ($^{GDMi}EC_{50}/R_{max}$)] was higher in GDM*i* (~18 fold) and GDM*d* (~13 fold), compared with vessel rings from normal pregnancies. This phenomenon could result from a lack of endothelial function since the response of vessels to CGRP was also reduced in GDM*i* (~10 fold). However, GDM*i* would be a stronger condition than GDM*d* generating endothelial dysfunction since CGRP response to insulin was ~7 fold higher than in GDM*d*.

In conclusion, HUVECs from GDM*i* pregnancies show increased L-arginine transport and NO synthesis, and reduced vascular reactivity compared with normal pregnancies. These findings are comparable to those in GDM*d*, suggesting that insulin therapy in pregnancy does not resolve the foetoplacental endothelial dysfunction associated with GDM pregnancies. However, since we used primary cultures of HUVECs and umbilical vein rings *in vitro*, our conclusions should not be taken as categorical. Insulin therapy normalizes maternal and foetal glycaemia [9,18,19], but nothing is reported regarding the potential effect of this intervention on foetus wellbeing [3,5]. Insulin therapy associates with higher frequency of complications in neonates [38], including larger chance to be born large for gestational age [39], larger number (~25%) of infants with one or more episodes with neonatal morbidity (neonatal asymptomatic hypoglycaemia) [40], and polyhydramnios [41], compared with infants born to mothers with GDM*d*. Since maternal insulin therapy effect in foetus development, newborn, and postnatal alterations are still unclear [3,5,9,42], maternal and neonatal complications are comparable in GDM*i* and GDM*d* [19,39], and insulin therapy seems not to revert GDM-associated foetoplacental endothelial dysfunction,

subjecting pregnant women with GDM to insulin therapy should be taken with caution since the risk of foetal health alterations.

Sources of funding

This work was supported by the Fondo Nacional de Desarrollo Científico y Tecnológico (FONDECYT) [grant numbers 1150377, 1150344, 11150083], Chile. Servicio de Salud de Medicina Oriente, Hospital San Juan de Dios [grant number Res. 1938–2016], Chile. This project has received funding from the Marie Curie International Research Staff Exchange Scheme with the 7th European Community Framework Program [grant agreement number 295185 - EULAMDIMA]. MS, LSi, RV-L, and RS hold Comisión Nacional para la Investigación en Ciencia y Tecnología (CONICYT) (Chile)-PhD fellowships. LSi and RS hold Vicerrectorate of Research and School of Medicine, PUC (Chile)-PhD fellowships. LSi holds UMCG University of Groningen Postgraduate School-PhD fellowship (The Netherlands).

Disclosures

None.

Transparency document

The http://dx.doi.org/10.1016/j.bbadis.2017.07.022 associated with this article can be found, in the online version.

Acknowledgements

Authors thank Mrs Amparo Pacheco from CMPL, Pontificia Universidad Católica de Chile (PUC), for excellent technical assistance.

References

[1] B.E. Metzger, Summary and recommendations of the Fifth International Workshop-Conference on Gestational Diabetes Mellitus, Diabetes Care 30 (2007) 251–560, http://dx.doi.org/10.2337/dc07-s225.
[2] M. Colomiere, M. Permezel, C. Riley, G. Desoye, M. Lappas, Defective insulin signaling in placenta from pregnancies complicated by gestational diabetes mellitus, Eur. J. Endocrinol. 160 (2009) 567–578, http://dx.doi.org/10.1530/EJE-09-0031.
[3] L. Sobrevia, R. Salsoso, T. Sáez, C. Sanhueza, F. Pardo, A. Leiva, Insulin therapy and fetoplacental vascular function in gestational diabetes mellitus, Exp. Physiol. 100 (2015) 231–238, http://dx.doi.org/10.1113/expphysiol.2014.082743.
[4] American Diabetes Association, Classification and diagnosis of diabetes. Section 2, Standards of Medical Care in Diabetes–2017, Diabetes Care, 40 2017, pp. S11–S24, , http://dx.doi.org/10.2337/dc17-S005.
[5] L. Silva, M. Subiabre, J. Araos, T. Sáez, R. Salsoso, F. Pardo, A. Leiva, R. San Martín, F. Toledo, L. Sobrevia, Insulin/adenosine axis linked signalling, Mol. Aspects Med. 55 (2017) 45–61, http://dx.doi.org/10.1016/j.mam.2016.11.002.
[6] A.B. König, S. Junginger, J. Reusch, F. Louwen, K. Badenhoop, Gestational diabetes outcome in a single center study: higher BMI in children after six months, Horm. Metab. Res. 46 (2014) 804–809, http://dx.doi.org/10.1055/s-0034-1375652.
[7] T.P. Waters, A.R. Dyer, D.M. Scholtens, S.L. Dooley, E. Herer, L.P. Lowe, J.J. Oats, B. Persson, D.A. Sacks, B.E. Metzger, P.M. Catalano, HAPO Cooperative Study Research Group, Maternal and neonatal morbidity for women who would be added to the diagnosis of GDM using IADPSG criteria: a secondary analysis of the hyperglycemia and adverse pregnancy outcome study, Diabetes Care 39 (2016) 2204–2210, http://dx.doi.org/10.2337/dc16-1194.
[8] K.J. Hunt, D.L. Conway, Who returns for postpartum glucose screening following gestational diabetes mellitus? Am. J. Obstet. Gynecol. 198 (2008) 404.e1-6, http://dx.doi.org/10.1016/j.ajog.2007.09.015.
[9] O. Verier-Mine, Outcomes in women with a history of gestational diabetes. Screening and prevention of type 2 diabetes. Literature review, Diabetes Metab. 36 (2010) 595–616, http://dx.doi.org/10.1016/j.diabet.2010.11.011.
[10] L. Hiersch, Y. Yogev, Management of diabetes and pregnancy—when to start and what pharmacological agent to choose? Best Pract. Res. Clin. Obstet. Gynaecol. 29 (2015) 225–236, http://dx.doi.org/10.1016/j.bpobgyn.2014.04.020.
[11] P.R. Olmos, A.P. Araya-Del-Pino, C.A. González-Carvello, P. Laso-Ulloa, M.I. Hodgson, V. Irribarra, G.R. Borzone, C. Belmar, A. Poblete, C. Berríos, J. Becker, C.M. Zajer-Amar, A. Manzur, M. Bozinovic, R.J. Miranda, A. Diez, H. Vidal, R. Ramírez-Armijo, R.I. Olmos, C. Tabilo, J. Ahuad, Near-optimal glycemic control in Chilean women with pregestational type-2 diabetes: persistent macrosomia relates to maternal pre-pregnancy overweight, Diabetes Res. Clin. Pract. 85 (2009) 53–60, http://dx.doi.org/10.1016/j.diabres.2009.04.015.
[12] F. Westermeier, C. Salomón, M. González, C. Puebla, E. Guzmán-Gutiérrez, F. Cifuentes, A. Leiva, P. Casanello, L. Sobrevia, Insulin restores gestational diabetes mellitus-reduced adenosine transport involving differential expression of insulin receptor isoforms in human umbilical vein endothelium, Diabetes 60 (2011) 1677–1687, http://dx.doi.org/10.2337/db11-0155.
[13] E. Guzmán-Gutiérrez, A. Armella, F. Toledo, F. Pardo, A. Leiva, L. Sobrevia, Insulin requires A1 adenosine receptors expression to reverse gestational diabetes-increased L-arginine transport in human umbilical vein endothelium, Purinergic Signal 12 (2016) 175–190, http://dx.doi.org/10.1007/s11302-015-9491-2.
[14] R. Devés, C.A. Boyd, Transporters for cationic amino acids in animal cells: discovery, structure, and function, Physiol. Rev. 78 (1998) 487–545.
[15] G.E. Mann, D.L. Yudilevich, L. Sobrevia, Regulation of amino acid and glucose transporters in endothelial and smooth muscle cells, Physiol. Rev. 83 (2003) 183–252, http://dx.doi.org/10.1152/physrev.00022.2002.
[16] F. Westermeier, C. Salomón, M. Farías, P. Arroyo, B. Fuenzalida, T. Sáez, R. Salsoso, C. Sanhueza, E. Guzmán-Gutiérrez, F. Pardo, A. Leiva, L. Sobrevia, Insulin requires normal expression and signaling of insulin receptor A to reverse gestational diabetes-reduced adenosine transport in human umbilical vein endothelium, FASEB J. 29 (2015) 37–49, http://dx.doi.org/10.1096/fj.14-254219.
[17] M. González, S. Rojas, P. Avila, L. Cabrera, R. Villalobos, C. Palma, C. Aguayo, E. Peña, V. Gallardo, E. Guzmán-Gutiérrez, T. Sáez, R. Salsoso, C. Sanhueza, F. Pardo, A. Leiva, L. Sobrevia, Insulin reverses D-glucose-increased nitric oxide and reactive oxygen species generation in human umbilical vein endothelial cells, PLoS One 10 (2015) e0122398, , http://dx.doi.org/10.1371/journal.pone.0122398.
[18] M.A. Hickman, R. McBride, K.A. Boggess, R. Strauss, Metformin compared with insulin in the treatment of pregnant women with overt diabetes: a randomized controlled trial, Am. J. Perinatol. 30 (2013) 483–490, http://dx.doi.org/10.1055/s-0032-1326994.
[19] M. Watanabe, A. Katayama, H. Kagawa, D. Ogawa, J. Wada, Risk factors for the requirement of antenatal insulin treatment in gestational diabetes mellitus, J. Diabetes Res. 2016 (2016) 9648798, http://dx.doi.org/10.1155/2016/9648798.
[20] MINSAL, Guía Perinatal 2015, Ministry of Health, Government of Chile, 2015.
[21] K. Howorka, Criteria for functional insulin treatment, in: Kinga Howorka (Ed.), Functional Insulin Treatment. Principles, Teaching approach and Practice, Springer-Verlag Berlin Heidelberg, Germany, 1996, pp. 78–99, , http://dx.doi.org/10.1007/978-3-642-79997-6.
[22] I. Fleming, R. Busse, Molecular mechanisms involved in the regulation of the endothelial nitric oxide synthase, Am. J. Phys. 284 (2003) R1–R12, http://dx.doi.org/10.1152/ajpregu.00323.2002.
[23] K.N. Aronis, J.P. Chamberland, C.S. Mantzoros, GLP-1 promotes angiogenesis in human endothelial cells in a dose-dependent manner, through the Akt, Src and PKC pathways, Metabolism 62 (2013) 1279–1286, http://dx.doi.org/10.1016/j.metabol.2013.04.010.
[24] C.M. Crews, R.L. Erikson, Purification of a murine protein-tyrosine/threonine kinase that phosphorylates and activates the Erk-1 gene product: relationship to the fission yeast byr1 gene product, Proc. Natl. Acad. Sci. U. S. A. 89 (1992) 8205–8209, http://dx.doi.org/10.1073/pnas.89.17.8205.
[25] M. González, V. Gallardo, N. Rodríguez, C. Salomón, F. Westermeier, E. Guzmán-Gutiérrez, F. Abarzúa, A. Leiva, P. Casanello, L. Sobrevia, Insulin-stimulated L-arginine transport requires SLC7A1 gene expression and is associated with human umbilical vein relaxation, J. Cell. Physiol. 226 (2011) 2916–2924, http://dx.doi.org/10.1002/jcp.22635.
[26] C. Salomón, F. Westermeier, C. Puebla, P. Arroyo, E. Guzmán-Gutiérrez, F. Pardo, A. Leiva, P. Casanello, L. Sobrevia, Gestational diabetes reduces adenosine transport in human placental microvascular endothelium, an effect reversed by insulin, PLoS One 7 (2012) e40578, , http://dx.doi.org/10.1371/journal.pone.0040578.
[27] L. Sobrevia, D.L. Yudilevich, G.E. Mann, Elevated D-glucose induces insulin insensitivity in human umbilical endothelial cells isolated from gestational diabetic pregnancies, J. Physiol. 506 (1998) 219–230, http://dx.doi.org/10.1111/j.1469-7793.1998.219bx.x.
[28] G. Vásquez, F. Sanhueza, R. Vásquez, M. González, R. San Martín, P. Casanello, L. Sobrevia, Role of adenosine transport in gestational diabetes-induced L-arginine transport and nitric oxide synthesis in human umbilical vein endothelium, J. Physiol. 560 (2004) 111–122, http://dx.doi.org/10.1113/jphysiol.2004.068288.
[29] A. Grupper, M. Shashar, D. Bahry, Y. Pri-Paz, O. Ben Tur, S. Levi, T. Chernichovski, G. Chernin, I.F. Schwartz, Cyclosporine attenuates arginine transport, in human endothelial cells, through modulation of cationic amino acid transporter-1, Am. J. Nephrol. 37 (2013) 613–619, http://dx.doi.org/10.1159/000350614.
[30] O.S. Bentur, T. Chernichovski, M. Ingbir, T. Weinstein, I.F. Schwartz, Dimethyl sulfoxide attenuates nitric oxide generation via modulation of cationic amino acid transporter-1 in human umbilical vein endothelial cells, Cryobiology 73 (2016) 226–231, http://dx.doi.org/10.1016/j.cryobiol.2016.07.006.
[31] J.S. Camelo Jr., S.M. Jorge, F.E. Martinez, Amino acid composition of parturient plasma, the intervillous space of the placenta and the umbilical vein of term newborn infants, Braz. J. Med. Biol. Res. 37 (2004) 711–717, http://dx.doi.org/10.1590/S0100-879X2004000500013.
[32] J. Wang, T. Kotani, H. Tsuda, Y. Mano, S. Sumigama, H. Li, K. Komatsu, R. Miki, E. Maruta, Y. Niwa, T. Mitsui, S. Yoshida, M. Yamashita, K. Tamakoshi, F. Kikkawa, Is the serum L-arginine level during early pregnancy a predictor of pregnancy-induced hypertension? J. Clin. Biochem. Nutr. 57 (2015) 74–81, http://dx.doi.org/10.3164/jcbn.14-104.
[33] M. González, C. Flores, J.D. Pearson, P. Casanello, L. Sobrevia, Cell signalling-mediating insulin increase of mRNA expression for cationic amino acid transporters-1 and -2 and membrane hyperpolarization in human umbilical vein endothelial cells, Pflugers Arch. 448 (2004) 383–394, http://dx.doi.org/10.1007/s00424-004-1261-x.
[34] R. San Martín, L. Sobrevia, Gestational diabetes and the adenosine/L-arginine/nitric

oxide (ALANO) pathway in human umbilical vein endothelium, Placenta 27 (2006) 1–10, http://dx.doi.org/10.1016/j.placenta.2005.01.011.
[35] P. Di Fulvio, A. Pandolfi, G. Formoso, S. Di Silvestre, P. Di Tomo, A. Giardinelli, A. De Marco, N. Di Pietro, M. Taraborrelli, S. Sancilio, R. Di Pietro, M. Piantelli, A. Consoli, Features of endotelial dysfunction in umbilical cord vessels of women with gestational diabetes, Nutr. Metab. Cardiovasc. Dis. 24 (2014) 1337–1345, http://dx.doi.org/10.1016/j.numecd.2014.06.005.
[36] I. Fleming, Molecular mechanisms underlying the activation of eNOS, Pflugers Arch. 459 (2010) 793–806, http://dx.doi.org/10.1007/s00424-009-0767-7.
[37] U. Förstermann, W.C. Sessa, Nitric oxide synthases: regulation and function, Eur. Heart J. 33 (2012) 829–837, http://dx.doi.org/10.1093/eurheartj/ehr304.
[38] Z. Fazel-Sarjoui, A. Khodayari Namin, M. Kamali, N. Khodayari Namin, A. Tajik, Complications in neonates of mothers with gestational diabetes mellitus receiving insulin therapy versus dietary regimen, Int. J. Reprod. Biomed. 14 (2016) 275–278.
[39] S.H. Koning, K. Hoogenberg, K.A. Scheuneman, M.G. Baas, F.J. Korteweg, K.M. Sollie, B.J. Schering, A.J. van Loon, B.H. Wolffenbuttel, P.P. van den Berg, H.L. Lutgers, Neonatal and obstetric outcomes in diet- and insulin-treated women with gestational diabetes mellitus: a retrospective study, BMC Endocr. Disord. 16 (2016) 52, http://dx.doi.org/10.1186/s12902-016-0136-4.
[40] B. Persson, M. Stangenberg, U. Hansson, E. Nordlander, Gestational diabetes mellitus (GDM). Comparative evaluation of two treatment regimens, diet versus insulin and diet, Diabetes 34 (1985) 101–105.
[41] D. Bogdanet, A.M. Egan, C. Reddin, O. Kgosidialwa, B. Kirwan, L. Carmody, F.P. Dunne, ATLANTIC DIP: insulin therapy for women with IADPSG-diagnosed gestational diabetes mellitus. Does it work? J. Clin. Endocrinol. Metab. 102 (2017) 849–857, http://dx.doi.org/10.1210/jc.2016-2911.
[42] L. Sobrevia, R. Salsoso, B. Fuenzalida, E. Barros, L. Toledo, L. Silva, C. Pizarro, M. Subiabre, R. Villalobos, J. Araos, F. Toledo, M. González, J. Gutiérrez, M. Farías, D.I. Chiarello, F. Pardo, A. Leiva, Insulin is a key modulator of fetoplacental endothelium metabolic disturbances in gestational diabetes mellitus, Front. Physiol. 7 (2016) 119, http://dx.doi.org/10.3389/fphys.2016.00119.